Academic Journal of Science and Technology
ISSN: 2771-3032 | Vol. 13, No. 2, 2024

Optimization and Verification of Sliding Saddle Structure in Machining Centers

Zhuolin Wen[1], Yun Xu[1, 2], Qi Li[2], Shuai Ye[1], Ling He[1]

[1]Mechanical Engineering Department, Sichuan University of Science & Engineering, Yibin 644000, China
[2]Sichuan Changzheng Machine Tool Group Co., Ltd., Zigong 643000, China

Abstract: As one of the key components of CNC machining centers, the structural performance of the saddle plays an important role in the machining accuracy of CNC machine tools. Taking the high-precision machining center of a certain factory as the research object, a finite element model of the sliding saddle is established. The ANSYS software is used to perform static analysis on the sliding saddle under extreme working conditions, analyze the deformation of the sliding saddle under this working condition, identify the weak links of the sliding saddle, and optimize its structure and size. Static stiffness verification and modal analysis verification are carried out. The results show that the optimized machining center saddle has high static stiffness and does not exhibit resonance under normal working conditions.

Keywords: Machining center; saddle; finite element analysis; modal analysis.

1. Introduction

The high-precision machining center is an indispensable processing equipment in the modernization development of the mechanical field. The casting part of the high-precision machining center mainly consists of the spindle box, column, bed, sliding saddle, and worktable, and its performance requirements are higher than those of ordinary machine tools. The sliding saddle is one of the important parts of the high-precision machining center[1], but it carries the worktable and the workpiece to be processed, and connects the X-axis and Y-axis movements. It is also one of the most easily deformed castings, and its dynamic performance has a decisive effect on the overall performance of the high-precision machining center. Once it deforms, it will directly affect the accuracy of the processed parts [2-5]. Therefore, in order to ensure that the high-precision machining center has good structural characteristics and processing accuracy, this paper will conduct static analysis and optimization of a high-precision machining center sliding saddle, and add vibration modal analysis, in order to obtain a sliding saddle model with the required performance.

In recent years, with the popularization of finite element-related software in design, civil engineering, mechanical engineering and other fields, domestic and foreign scholars have mostly begun to use finite element method for structural optimization and analysis verification of various parts of machine tools. Su Yufeng [6] used finite element method to conduct structural design and optimization of a certain type of machining center's saddle, Li Jie [7] used finite element method to conduct structural optimization and analysis of a certain high-speed milling bed saddle. Hung Sun [8] studied the dynamic characteristics of machine tools through finite element analysis and a series of dynamic experiments. He analyzed the influence of vibration effects on product accuracy while giving corresponding solutions. Altintas [9] analyzed the dynamic characteristics of various parts of machining centers under various working conditions and simulated the possible vibratory effects of machining centers during operation.

In this design, the finite element method and ANSYS related software will also be used to establish a finite element model for the sliding saddle of the machining center, and the part of the sliding saddle castings will be analyzed by statics to obtain the stress-strain conditions and stress deformation conditions of the castings, which will provide an important theoretical basis for the subsequent design and verification of the sliding saddle structure[10-11].

2. The Establishment and Simulation of Finite Element Model

2.1. Establishment of finite element model of sliding saddle

In this study, the 3D modeling software SolidWorks was used to establish the 3D model of the sliding saddle of the high-precision machining center. The maximum x dimension of the sliding saddle was 1900mm, and the center distance between the two sliding rails at the joint of the sliding saddle and the workbench was 322mm. Before the saddle is imported into the finite element software for analysis, it should be considered to simplify the structure of the existing saddle model. This simplification will consider removing some features including threaded holes, rounded corners and chamfer. The 3D model of the saddle after simplification is shown in Figure 1.

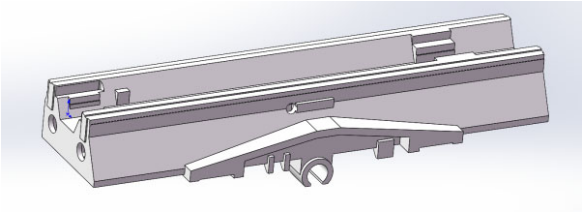

Figure 1. Simplified diagram of saddle model

The simplified model was imported into the finite element software ANSYS Workbench for analysis. Before dividing the grid of the sliding saddle model, it is necessary to give the model various material properties first. The selection of parameters of sliding saddle materials is shown in Table 1.

Table 1. Saddle material parameter

Material Parameters	Parameter size
Saddle material	HT250 gray pig iron
Density	7280kg/m³
Elasticity modulus	1.38×10¹¹Pa
Poisson's ratio	0．156

In this simulation, due to the complex structure of the saddle, the solid187 tetrahedral element is considered in the grid division, and the grid division of the finite element model of the saddle is completed by free grid division. This type of element can fully meet the requirements of calculation accuracy. The sliding saddle after grid division is shown in Figure 2. A total of 2,232,069 nodes and 1,304,829 units are divided.

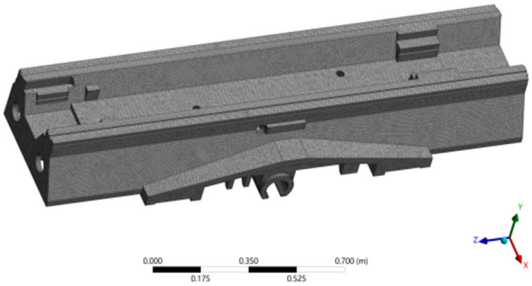

Figure 2. Diagram of the finite element model of the saddle

2.2. Simulation analysis of sliding saddle

Static analysis is used in this analysis, which mainly calculates the maximum static deformation of the saddle under the action of various forces. In order to facilitate the analysis, the position deviation constraint of the saddle is set on the contact surface between the saddle and the slide rail on the base. It should be noted that although there must be a gap between the contact surface of the sliding saddle and the guide rail of the base in actual working conditions, the analysis here only adopts static analysis and does not consider the analysis of the dynamic characteristics of the sliding saddle. Therefore, the full constraint load can be directly applied on the contact surface of the sliding saddle and the sliding rail on the base. Firstly, when the table moves to the position where the saddle is most likely to deform, that is, to the limit position of the saddle X in the positive direction and the limit position of the saddle X in the negative direction, the influence of the table gravity, the maximum work piece load, the cutting force and the gravity of the saddle on the deformation of the saddle on the contact surface between the saddle and the table is studied. At the same time, considering the influence of the same force load when the table is moved to the middle position of the sliding saddle, the deformation characteristics of the sliding saddle under different working conditions can be better understood by comparing with the previous two working conditions. Each load is added to the corresponding position of the above three working conditions in the form of distributed load, and each load is the maximum value, among which, the gravity of the workbench is 4800N, the maximum load of the workbench is 8000N, the cutting force is 1000N, the self-weight load of the sliding saddle is 5100N, the gravitational acceleration is 9.81m/s2, and the direction is vertical downward. After applying the above load to the corresponding position of the saddle surface in ANSYS software, the corresponding deformation result of the saddle can be obtained.

3. Result Analysis and Optimization Design

3.1. Result analysis

After the completion of ANSYS calculation, the cloud map of the combined displacement field distribution of the sliding saddle in three positions can be obtained from the results of ANSYS analysis and calculation, as shown in Figure 3.

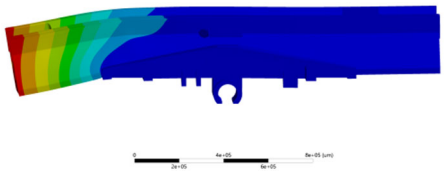

(a) Table in the saddle X positive limit position

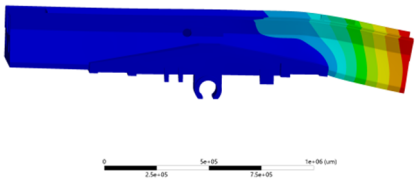

(b) Table in saddle X negative direction limit position

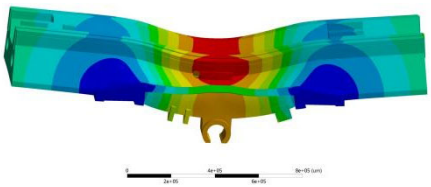

(c)Table in the middle of the saddle

Figure 3. Contour of the combined displacement field distribution of the saddle at three positions

By analyzing the deformation situation as shown in FIG. 3, the movement of the table with full load to three different positions relative to the sliding saddle, that is, the maximum deformation situation of the sliding saddle under three different working conditions, was recorded respectively, and the results were shown in Table 2.

Table 2. The maximum deflection of the saddle under three operating conditions

Table position	Table in the saddle X positive limit position	Table in saddle X negative direction limit position	Table in the middle of the saddle
maximum deformation (μm)	18.784	14.9	5.741

According to the data in Table 2, when the table moves to the limit position of the saddle X in positive and negative directions, the load on the saddle is similar to the force mechanism of the cantilever beam, which makes the maximum deformation of the saddle in the above working conditions significantly increase, far exceeding that in other positions. In order to eliminate the adverse effects caused by the deformation and ensure the stability of the processing

process, the existing structure of the sliding saddle must be optimized to reduce the maximum deformation of the sliding saddle when the table moves to the limit position on both sides of the sliding saddle. This design adopts the method of increasing the rib plate inside the sliding saddle and adjusting the structure of the internal reinforcement at both ends of the sliding saddle with the largest deformation.

3.2. Optimization design

After adjusting the internal structure of the sliding saddle, the structure comparison of the sliding saddle is shown in Figure 4.

(a) Original saddle structure (part)

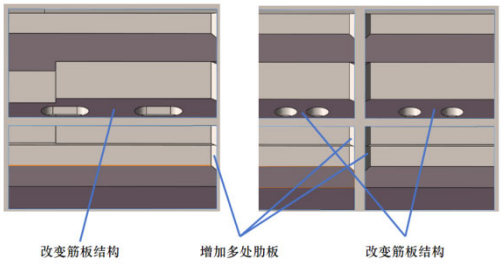

(b) The optimized structure of the saddle (part)

Figure 4. Optimized the comparison of the front and rear saddle structures

After optimizing the structure of the sliding saddle as shown in the figure above, the new structure of the sliding saddle was re-introduced into the finite element software ANSYS Workbench for analysis, keeping the position and size of each load unchanged. The results show that the deformation of the new sliding saddle structure is still vertical downward, but compared with the old structure, the maximum deformation of the new sliding saddle structure is significantly improved. The maximum deformation of the new saddle structure is shown in Table 3.

Table 3. The maximum amount of deformation of the new saddle structure

Table position	maximum deformation (μm)	Compared with before optimization
Table in the saddle X positive limit position	15.389	-18.07%
Table in saddle X negative direction limit position	11.798	-20.82%

4. Optimization Result Verification

4.1. Static stiffness verification

After the above optimization of the structure of the saddle, its static stiffness will be verified. Through the comparison before and after the design, it is found that the weight of the sliding saddle increases by 0.23%. At the same time, when the table moves to the positive and negative limit position of the sliding saddle X with full load, the maximum deformation on both sides of the sliding saddle is reduced by about 19.5%. After structural optimization, the change of the maximum deformation of the sliding saddle in the motion stroke of the table is significantly reduced, which indicates that the stability and reliability of the sliding saddle have been improved. The static stiffness of the saddle structure is significantly improved, which ensures the overall machining quality. In addition, the increase of static stiffness is not only beneficial to the static performance of the saddle, but also has a positive impact on its dynamic performance. According to Table 3, the maximum deformation of the sliding saddle when the workbench is in the limit working condition can be obtained, and the static stiffness of the sliding saddle itself can be calculated [12]. Here, the deformation when the workbench moves to the limit position of the sliding saddle X in the positive direction, that is, 15.389μm, is selected for calculation. Therefore, the static stiffness of the new saddle structure is:

$$K = P/Y = 13800/15.398 = 896\ N/\mu m \quad (1)$$

After the calculation, the static stiffness of the saddle structure is increased to 896N/μm, which verifies the rationality of the optimization of the saddle structure.

4.2. Modal analysis verification

the natural frequency and mode of the structure, so as to provide an effective basis to avoid the occurrence of resonance phenomenon. For the machining center, the dynamic performance of the sliding saddle has a crucial impact on ensuring the machining accuracy. In this analysis, the ANSYS software family will continue to be used. Modal analysis in the ANSYS product family is a linear analysis, and any nonlinear characteristics, even if defined, will be ignored [13]. In order to solve the dynamic characteristics of the sliding saddle, the block Lanczos algorithm, one of the seven mode extraction methods provided by ANSYS products, is selected here. Block Lanczos algorithm is an iterative algorithm. The eigenvalues and eigenvectors are obtained by iterating the input matrix. Compared with the traditional direct solution method and the traditional subspace method, the partitioning Lanczos algorithm has higher solving efficiency and lower computing cost, and is especially suitable for large complex structure models. The model belongs to a large and complex structure, so the natural frequency and vibration mode of the sliding saddle can be solved quickly and accurately by using this extraction method.

In general, for dynamic analysis, each mode represents the vibration mode of the structure at different frequencies, and the mode of lower frequency corresponds to the main vibration mode of the structure, which has a larger amplitude and a wider energy distribution, and therefore has a greater impact on the structural response. That is, the lower the modal frequency of the structure, the greater the weight of the modal in the structural response. This is because the low frequency modes play an important role in the overall vibration characteristics and energy transfer of the structure. In other words, the low-order modal characteristics basically determine the dynamic characteristics of the product [14], so this verification will focus on the first four order natural

frequencies of the saddle. Since this modal analysis is a linear analysis, only the fully constrained load can be applied for constraint, and the fully constrained load is chosen to be applied at the junction between the saddle and the slide rail, that is, UX=UY=UZ=0[15]. After the fully constrained load is applied, the first four natural frequencies and vibration modes of the sliding saddle are shown in Table 4, and the modes of the first four modes are shown in Figure 5.

Table 2. Saddle natural frequencies and mode shapes

Frequency order	Frequency/Hz	mode of vibration
1	176	The sliding saddle is rotated clockwise around the Y-axis, and the deformation is greatest in the positive limit position of the X-axis
2	189	Both sides of the saddle are tilted upward, and the X-axis negative limit position deformation is the largest
3	204	Both sides of the saddle are pressed down, and the X-axis positive limit position deformation is the largest
4	222	The sliding saddle is twisted counterclockwise along the X-axis, and the deformation is greatest at the limit position in the negative direction of the X-axis

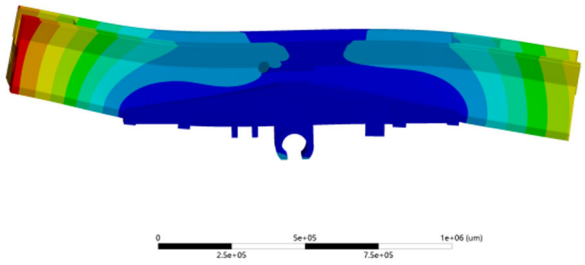

(a) First order mode diagram of the saddle

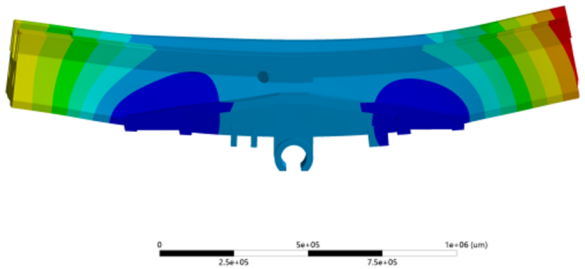

(b) Second order mode diagram of the saddle

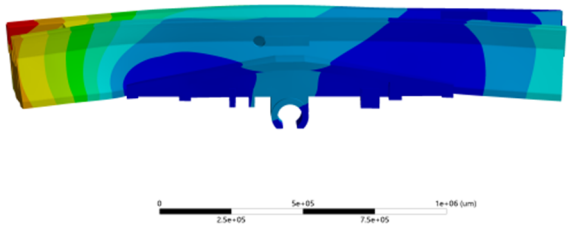

(c) Third order mode diagram of the saddle

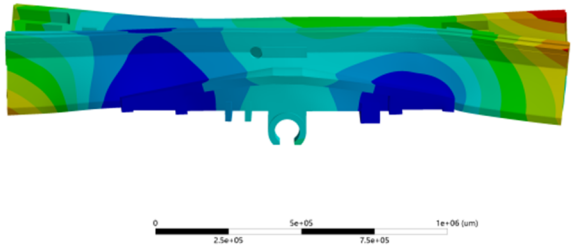

(d) Fourth order mode diagram of the saddle

Figure 2. Diagram of the fourth-order mode shape before the saddle

According to the design requirements of the machine tool, the maximum speed of the table moving on the sliding saddle is 40m/min, and the pitch of the sliding saddle screw commonly used on the market is 8, 10, 12, 16, 20mm. According to the working characteristics of the screw with large load and high speed, a screw with a pitch of 16mm is considered. The choice of this lead screw can also reduce the motor load, reduce heat generation, and reduce losses. From this, the limit speed of the motor can be obtained:

$$n = S/P = 2500\,r/min \tag{2}$$

Then the maximum exciting frequency of the saddle can be calculated：

$$f = n/60 = 41.7Hz \tag{3}$$

It can be seen from Table 4 that the first four natural frequencies of the sliding saddle are as low as 176Hz and as high as 222Hz, both of which are far higher than the maximum exciting frequency of the sliding saddle of 41.7Hz. Therefore, under normal working conditions, the sliding saddle will definitely not produce resonance phenomenon[16]。

By analyzing the vibration pattern of the saddle derived from ANSYS software, it can be concluded that the limit positions of the left and right sides of the saddle are the weak positions of the saddle, and the preliminary conclusion is that under normal working conditions, the force structure of the left and right limit positions is similar to the bending deformation caused by the cantilever beam. In the follow-up study, if we want to further optimize the sliding saddle of the machining center, we can consider making corresponding adjustments to these structures.

5. Conclusion

For a sliding saddle in a machining center, the static stiffness analysis was carried out by using ANSYS finite element software, and then the corresponding optimization measures were taken to improve the static stiffness of the sliding saddle. When the mass of the sliding saddle was increased by 0.023%, the maximum deformation of the sliding saddle at the limit condition was reduced by 20%, which ensured the smoothness of the table moving on the sliding saddle. Meet the established design requirements. In the follow-up verification, the static stiffness verification and modal analysis verification of the new structure of the sliding saddle were carried out, and the static stiffness was calculated to be 896N/μm, and the first four natural frequencies obtained

by the analysis and calculation were much higher than the maximum exciting frequency of the sliding saddle, thus verifying the rationality of the structure optimization. At present, after the completion of the structure optimization of the saddle, the saddle has been manufactured in the factory according to the actual improvement, and will be applied to the actual working conditions, the next step will be verified by practical application, so that the design and manufacturing of the saddle has been effectively confirmed, providing strong support for the future development of similar engineering projects. The actual assembled sliding saddle and some of its accessories are shown in Figure 6.

Figure 6. The actual assembled saddle and some of its accessories

Acknowledgments

Foundation item: Zigong Science and Technology Bureau project "Aviation Five-axis bridge gantry processing equipment development" (2022CD ZG-19)

Cited References

[1] Qi Jibao, Yang Weimin. Geometric error compensation method of NC machine tool based on differential variation construction method [J]. Transactions of Agricultural Machinery, 2016, 47(9): 398－405.

[2] Lei Yonghong, Wang Meng. Discussion on technological improvement of machine tool sliding saddle castings [J]. Casting Equipment And Technology, 2022, (04):22-24.

[3] Zhao Lei. Static analysis and structural optimization of sliding saddle of horizontal turn-milling complex machining center [J]. Mechanical Engineer,2023,(12):129-131.

[4] Zhu Zanbin, Li Meng, FENG Shijie. Improved design and statics analysis of sliding saddle for 5-axis machining center [J]. Manufacturing Technology & Machine Tool, 2020,(03):43-46.

[5] Zhu Jun. Saddle mechanism design of high speed precision CNC machine tool based on finite element analysis [J]. Mechanical Design and Manufacturing Engineering, 2020, 49(04): 46-50.

[6] Su Yufeng, Yuan Wenxin, Liu Deping, et al. Thermal characteristics analysis of bed saddle in high speed turning and milling complex machining center [J]. Combined Machine Tools and Automated Processing Technology, 2011,(4) : 31-32,36.

[7] Li Jie, Liu Deping, Su Yufeng, et al. Temperature field modeling and thermal deformation analysis of saddle for high speed milling machine[J].Machinery Design and Manufacture, 2011, (7) : 211-212.

[8] Hungsun S, Choi H J, Park H W.Design and dynamic analysis of an arch-type desktop reconfigurable machine [J]. International Journal of Machine Tools and Manufacture, 2010, 50(6) : 575-584.

[9] Altintas Y，Stepan G，Merdol D，et al． Chatter stability of milling in frequency and discrete time domain[J].CIRP Journal of Manufacturing Science and Technology,2008,1(1) : 35-44.

[10] Wang Yanning, Gao Yue. Structural Stiffness analysis and lightweight design of machine tool based on finite element method[J].Equipment Machinery,2023,(04):30-32+59.

[11] Li Qi, ZHAO Yan, Fang Hui, et al. Finite element analysis and structure optimization of five-axis CNC tool grinding machine [J]. Combined Machine Tools and Automated Processing Technology, 2023,(05):169-173.

[12] Yang Xiaojing, Chen Zichen, Liu Jianxiong, et al. Optimization design of key parts of XK640 CNC milling machine based on ANSYS static stiffness analysis[J].Machine Tool & Hydraulics,2007,(09):42-45.

[13] Xu Kaiyuan, Xu Wubin, TANG Manbin. Dynamic characteristic analysis of machine tool sliding saddle structure based on finite element method [J]. Machinery Design and Manufacture, 2011,(04):170-172.

[14] Tang Wencheng, Yi Hong, Xing Yan. Structure analysis of machining center bed[J].Mechanical Strength,1998 (1) : 13－15,20.

[15] Qin Wenhao, Zuo Zhengxing. Dynamic characteristic analysis of machine tool [J]. Machine Design, 2000 (24): 24-26.

[16] Chen Weiguo, Zhao Suna. Resonance suppression analysis of CNC machine tool servo shaft based on FANUC [J]. Automation Technology and Application, 2011, 30(09): 42-45.